Environmental Earth Sciences (2018) 77:40
https://doi.org/10.1007/s12665-017-7221-5

ORIGINAL ARTICLE

Integrated modelling for water quality management in a eutrophic reservoir in south-eastern Portugal

David Brito[1] · Tiago B. Ramos[1] · Maria C. Gonçalves[2] · Manuela Morais[3] · Ramiro Neves[1]

Received: 28 March 2017 / Accepted: 30 December 2017 / Published online: 19 January 2018

Abstract

The Enxoé Reservoir was built in 1998. Since 2000, it has exhibited frequent high chlorophyll-*a* concentrations, reaching a geometric mean three times higher than the national limit for eutrophication, presenting the reservoir with the highest eutrophic state in Portugal. Toxic algal blooms have also often been observed, which pose serious challenges to water managers, as the reservoir is used for potable water production (25,000 inhabitants). The objective of this study was to implement a reservoir model (CE-QUAL-W2), with inputs from a watershed model (SWAT), in order to represent the actual reservoir state and to test management measures to reduce its trophic level and algal bloom concentration peaks. The integrated model was used to depict the origin of its trophic status. Simulations were also compared to measured data at the reservoir surface (water level, nitrate, orthophosphate, suspended solids, and oxygen) and in water profiles (temperature, oxygen). The model was able to represent stratification and thermocline depths, as well as the actual chlorophyll-*a* and dissolved oxygen concentrations. The model results showed that internal phosphorus load from deposited sediments was an important factor in fuelling the algal blooms. This process occurs predominantly in summer, when stratification takes place and aeration is reduced, promoting anoxic conditions in the bottom waters. Since the reservoir is relatively shallow (average 5 m), released phosphorus is then easily able to reach the photic zone in most parts of the reservoir, where it is consumed. Different management scenarios were tested, suggesting that a mesotrophic level could barely be reached and maintained simply by reducing the nutrient loads (both external and internal). It is suggested that only an increase in the reservoir dam height could produce a mesotrophic level, averting anoxia by blocking the release of phosphorus from sediments to the photic zone. Future work should focus on a cost–benefit analysis to test the feasibility of each of the proposed scenarios, taking advantage of the integration strategy to assess where in the watershed load reductions would be most effective.

Keywords Eutrophic reservoir · Integrated modelling · CE-QUAL-W2 · SWAT · Phosphorus

Introduction

Enxoé is a temporary river watershed, limited downstream by a dam that was built in 1998. Since 2000, the reservoir has been exhibiting the highest eutrophic state in Portugal, registering frequent yearly chlorophyll-*a* concentrations greater than 50 μg L^{-1}, with maxima reaching 200 μg L^{-1}. The geometric average of surface chlorophyll-*a* concentration also reached 33 μg L^{-1} during 2001–2011, whereas the national limit for eutrophication is 10 μg L^{-1}.[1] Moreover, toxic cyanobacteria blooms have occurred (INAG 2004; Valério et al. 2005), interrupting water distribution to the local population. This constitutes a serious problem for water management, with constant reservoir eutrophication, particularly the presence of toxic algae in a reservoir used for potable water production, calling for improved management plans in the scope of the Water Framework Directive.

✉ David Brito
odavidbrito@gmail.com

[1] MARETEC, Instituto Superior Técnico, Universidade de Lisboa, Av. Rovisco Pais, 1049-001 Lisbon, Portugal

[2] Instituto Nacional de Investigação Agrária e Veterinária, Quinta do Marquês, Av. República, 2784-505 Oeiras, Portugal

[3] Laboratório da Água, Universidade de Évora, Rua da Barbarrala, 1, Parque Industrial e Tecnológico, 7000 Évora, Portugal

[1] The Portuguese trophic level classification was chosen, adapted from Organisation for Economic Co-operation and Development (OECD). The geometric average is used to reduce the weight of extreme values.

Cyanobacterial dominance is usually controlled by two main processes: some species are able to consume N_2 dissolved in the water (Paerl et al. 2001; Havens et al. 2003; Rolff et al. 2007), while others are further able to maintain growth, even under conditions of low light availability (Havens et al. 2003). The nitrogen fixation characteristics of some types of cyanobacteria further allow them to be independent of the availability of inorganic forms of nitrogen (e.g. ammonia, nitrate). Under conditions of nitrogen limitation, these species have then the potential to generate blooms if phosphorus is available (Havens et al. 2003).

Such a cyanobacterial response to phosphorus availability may have occurred in the Enxoé Reservoir after 2002, with species identified in 2003 and 2005 (Valério 2008). Previous studies have linked the cyanobacterial blooms in this reservoir to nutrient input loads from the watershed and hypothesized that such blooms could be associated with phosphorus inputs (Ramos et al. 2015a, b; Brito et al. 2017a, b). Those authors considered that phosphorus feeding from the watershed may have fuelled a process of both a fast and a delayed response in the reservoir, where initial blooms arose from the consumption of input dissolved nutrients, while later blooms were attributable to sediment sources, e.g. mineralization and desorption under anoxic conditions (Coelho et al. 2008).

A more comprehensive approach was required to fully understand the main physical and biochemical processes related to the eutrophication of the Enxoé Reservoir. One viable option was to integrate the watershed and reservoir, in order to determine the impact of management practices on the reservoir. Examples of such integrations have been given by Liu et al. (2015), who linked the SWAT (Neitsch et al. 2002) and CE-QUAL-W2 (Cole and Wells 2011) models to estimate nitrogen retention in the Shanmei Reservoir, China. Mateus et al. (2014) used those same models to determine management measures that could reduce the trophic level of the Tâmega Reservoir, Portugal. Debele et al. (2008) also implemented SWAT and CE-QUAL-W2 in determining their feasibility to represent hydrodynamic and water quality observations in the Cedar Creek Reservoir, USA. Xu et al. (2007) did the same with the HSPF and CE-QUAL-W2 models in the Occoquan watershed, USA. These integrated approaches have proved useful in representing the actual water body status and in testing the impact on the reservoir of the proposed management changes.

The SWAT model has been widely applied to a large range of watershed sizes and configurations to simulate flow and nutrient export on daily, monthly and annual scales (Gassman et al. 2007; Zhang et al. 2008). Examples of SWAT implementation in watersheds with similar sizes and land uses as Enxoé include the works of Geza and McCray (2008) and Green and van Griensven (2008) both in the USA, Yevenes and Mannaerts (2011) in Portugal, and Dechmi et al. (2012) and Panagopoulos et al. (2011) in Spain and Greece, respectively. The CE-QUAL-W2 model is widely applied for describing hydrodynamics and water quality in reservoirs, estuaries, and rivers (Kurup et al. 2000; Lung and Bai 2003; Makinia et al. 2005; Martin et al. 2013).

Here, a state-of-the-art modelling integration tool was applied, combining the best knowledge of the watershed and the reservoir to improve water quality management. The objective was to couple a watershed model (SWAT) and a reservoir model (CE-QUAL-W2), by integrating the available field data, in order to determine the origin of the Enxoé Reservoir eutrophication and to test best-suited management strategies (in the watershed and reservoir) to reduce its trophic status. This study complements a series of modelling studies aimed at improving water management plans in the Enxoé basin.

Materials and methods

Study site

Enxoé is a 60-km^2 catchment located in south-eastern Portugal, on the left margin of the Guadiana River (Fig. 1). The Enxoé River has a bed length of approximately 9 km, from its headwaters to the dam. The reservoir (37°59′38.121″N, 7°27′54.776″W) has a total volume of 10.4 hm^3, a surface area of approximately 2 km^2, an average depth of 5 m (maximum depth of 17 m near the dam), and an average residence time of 2 years. The reservoir level fluctuates 1–2 m from the maximum in wet years and 4–6 m in dry years (e.g. 2006 and 2008). The reservoir also exhibits a high algal and suspended solids content for most of the year, with Secchi disc depths around 1–3 m, creating thermal stratification during spring that lasts until winter, when higher flows and wind occur. Chlorophyll concentrations usually peak in the autumn (when flow and nutrient inputs from the watershed start, while the reservoir water temperatures are still relatively high) and in the summer (usually higher, due to high temperatures and low turbidity).

The climate in the region is dry sub-humid to semi-arid, with temperatures averaging 16 °C, and ranging from − 5 °C in winter to nearly 40 °C in summer. The precipitation regime is characterized by highly irregular behaviour, varying between relatively abundant rainfall episodes, concentrated in only a few minutes or hours, and frequent drought episodes, that can last from a few months to a couple of years. The annual average precipitation is 500 mm, irregularly distributed throughout the year. (80% of the annual precipitation is concentrated between October and April.) As a result, the river exhibits relatively large flow in the winter, as a response to rain events (up to 2 hm^3 $month^{-1}$), reduced flow in the spring after the rains cease, and no flow,

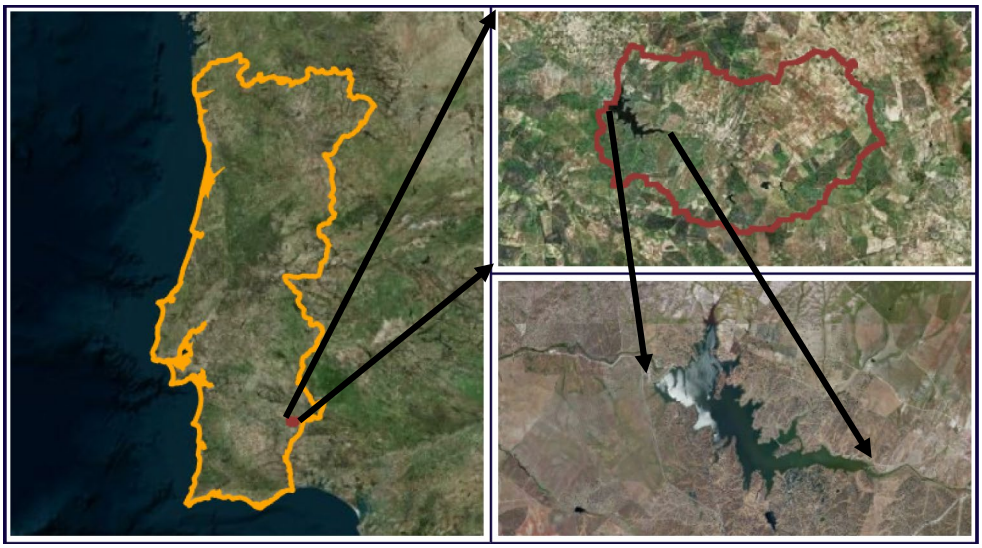

Fig. 1 Location of the Enxoé watershed in Portugal (left) and Enxoé Reservoir in the watershed (right)

with pool formation, during the summer or extended drought periods (Ramos et al. 2015a). The slopes are gentle, with an average river slope of approximately 2%, while the watershed shows an average slope of 5–6%. The gentle slopes promote water pooling and the occurrence of disconnected flow. The average maximum hourly wind is 2 ms^{-1}, reaching maxima of 20 ms^{-1}.

The soils in Enxoé originate mainly from granite and limestone (each contributing approximately 30% to the total area) and schist (with approximately 10% of the total area). The land is mainly used for growing olive trees, agroforestry of holm oaks ('montado'), and annual rainfed crops (wheat, oats, and sunflowers), each covering approximately 30% of the total area. Extensive livestock production is the most important animal-farming activity in the catchment. According to the 1999 agricultural census (INE 2001), cow (602) and sheep (4365) production each corresponded to approximately 0.1 livestock units per ha of agricultural surface. The catchment has a population of 1000 inhabitants, mainly concentrated in Vale de Vargo. The local wastewater treatment plant has discharged outside the watershed since 2006, as a protective measure to the Enxoé Reservoir. The reservoir currently supplies the villages of Mértola and Serpa with drinking water (25,000 inhabitants).

Modelling approach

Study background

The Enxoé watershed is small (60 km^2), and the river exhibits a flash flood regime that has never been studied in detail before. There has been a need for assessing both the long-term (annual nutrient and suspended sediment loads) and short-term (flash flood loads) inputs to the reservoir, in order to understand the watershed dynamics and their effects on the reservoir's trophic level.

Two approaches were considered: (1) long-term loads were estimated with the SWAT model (Neitsch et al. 2002), by comparing model predictions of flows and loads with recorded reservoir inflows and discrete sampling measurements, respectively (Brito et al. 2017a), and (2) short-term loads were assessed by applying the MOHID-Land model (Neves 2013) for predicting continuous probe measurements obtained during flash flood events (Brito et al. 2017b).

The two models have different structures that are particularly suitable for those purposes. SWAT is a semi-empirical model, with highly developed crop and management modules that use sub-basins for reservoir balance, and daily time-steps, making it adequate to run for long periods (e.g. years, decades), but failing in the detailed description of flash floods and related processes that occur in Enxoé in just a couple of hours. On the other hand, MOHID-Land is a physically based and distributed model with variable time-steps (of the order of seconds, or less, during intense fluxes, such as floods), being thus able to describe flash flood formation and propagation.

SWAT estimates of Enxoé long-term nitrogen loads reached 2.5–2.8 kgN ha^{-1} $year^{-1}$ (28 tonN $year^{-1}$), total suspended solids (TSS) loads were 0.45 ton ha^{-1} $year^{-1}$, and phosphorus loads were 0.3 kg ha^{-1} $year^{-1}$ (0.6 tonP $year^{-1}$). These estimates were comparable with those found in similar extensive agricultural areas, with gentle slopes (low erosion) and reduced human presence (Brito et al. 2017a).

MOHID-Land results, validated with field data taken during low-water and flood events over the course of 2 years, showed that, by considering the flood dynamics, the effective

Table 1 Summary comparison of SWAT model results to the collected data in the Enxoé watershed

Parameter	Period	Data average	Model Average	RMSE	R^2	Nash–Sutcliffe model efficiency
Flow						
Monthly reservoir inflow	1996–2009	0.24 hm^3 $month^{-1}$	0.24 hm^3 $month^{-1}$	0.21 hm^3 $month^{-1}$	0.78	0.77
River water quality						
Monthly total *N* load	2010–2011	0.62 tonN $month^{-1}$	0.50 tonN $month^{-1}$	0.46 tonN $month^{-1}$	0.69	0.65
Monthly total *P* load	2010–2011	0.034 tonP $month^{-1}$	0.030 tonP $month^{-1}$	0.025 tonP $month^{-1}$	0.63	0.62

annual phosphorus transport to the reservoir could be up to three times the average annual phosphorus load estimated by SWAT; in an average year, that would be 1.8 tonP $year^{-1}$. Also, the MOHID-Land and SWAT estimates of phosphorus loads reaching the drainage network were very similar (1.8 tonP $year^{-1}$); however, SWAT then considered that only 0.6 tonP $year^{-1}$ would reach the reservoir, with the remainder being deposited on the riverbed. On the other hand, the MOHID-Land results showed that the deposited material would later be resuspended during floods and would thereby also reach the reservoir (Brito et al. 2017b). Despite that, the SWAT model estimates were used in this study to feed the reservoir, since MOHID-Land simulated only the hydrodynamics. The extra phosphorus load that reached the reservoir—that was not described by SWAT—was used to proxy the actual situation of internal phosphorus load (see 'CE-QUAL-W2 model calibration/evaluation' section).

Models description

The SWAT model SWAT (Neitsch et al. 2002) implementation in the Enxoé catchment has already been described in detail in Brito et al. (2017a). Thus, only a brief description of the model setup will be given here. SWAT is a river basin model developed at Texas A&M University, wherein the land hydrodynamics component solves the water balance, relating meteorological variables to basin features (topography, soil type, and land use). For water quality assessment, the model further simulates plant growth, nitrogen and phosphorus soil cycles, and sediment and pesticides transport (Neitsch et al. 2002). The river outputs, that served as inputs to CE-QUAL-W2, were the nitrogen and phosphorus pools (dissolved forms as nitrate, ammonia, orthophosphate), organic matter, suspended solids, and oxygen.

In Enxoé, SWAT implementation was defined with 65 sub-watersheds and 161 hydrological response units, in order to describe the land use and soil distribution of the base data maps. These included NASA SRTM, with 3 arc seconds for the digital terrain model, CORINE land cover for land use, the European soil geographical database at 1:1,000,000 scale for soil texture, and the meteorological stations of the Portuguese Environmental Agency's (APA) network for weather data. The agricultural practices (crop rotation, fertilization) were obtained from farmer questionnaires and consisted of rotations between wheat and oats, and between sunflowers, wheat, and oats. Annual fertilization loads ranged from 40 to 90 and 20 kgP ha^{-1} $year^{-1}$ (Ramos et al. 2015a; Brito et al. 2017a). Animal nutrient production was obtained from the National Institute of Statistics (INE 2001). The annual animal loads were distributed homogeneously among the sites, with agroforestry of holm oaks, pasture (sheep and cattle), and olive trees (sheep), and throughout the year, following the extensive regime of animal production in Enxoé.

SWAT model implementation used the default boundary and initial conditions, including groundwater loss to the deep aquifer, drainage network outflow, and meteorological input data from recorded meteorological stations. Model calibration consisted of adjusting the hydraulic parameters that control the travel time of water between the soil and the aquifer, and the aquifer and the river, since these were shown to be relevant when modelling small, temporary river watersheds with small travel times and fast rise and fall hydrographs. In terms of water quality, in-stream rates were changed to represent the in-pool processes that occur in Enxoé after rain events cease, river water disconnections, due to temporary pool formation, and high retention times. Further details can be found in Brito et al. (2017a). A summary comparison of the SWAT results with the field data, in terms of monthly inflow and nutrient loads (field monitoring was put in place over a two-year period) is also presented in Table 1. Goodness-of-fit indicators, such as R^2 and Nash–Sutcliffe efficiency, varied between 0.62 and 0.8, showing a good model performance. The SWAT model represented a daily time-step, while the CE-QUAL-W2 model was variable, of the order of minutes. Thus, while daily input may not have described the short-term influence of fast floods, the important seasonal pattern and main nutrient input to the reservoir were described satisfactory by SWAT (reinforced by the results summarized in Table 1). The short-term pattern associated with the role of floods in load transport to

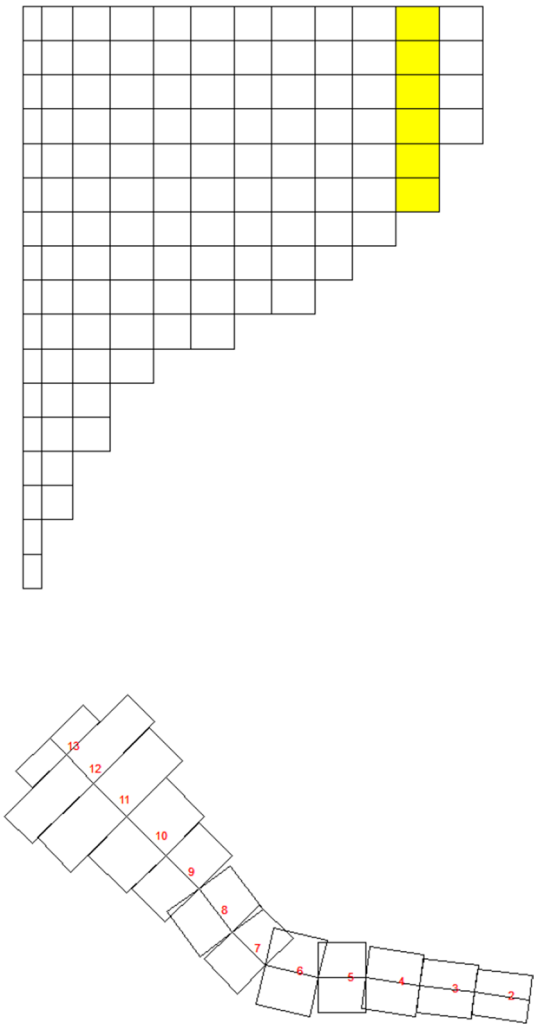

Fig. 2 CE-QUAL-W2 grid definition for Enxoé in plan view (bottom) and profile view (top) along the axis

the reservoir was addressed using the variable time-step model, MOHID-Land (Brito et al. 2017b).

The CE-QUAL-W2 model The CE-QUAL-W2 model (Cole and Wells 2011) version 3.7 was used for simulating the water quality in the Enxoé Reservoir. CE-QUAL-W2, developed by the US Corps of Engineers, is a bidimensional, laterally averaged, dynamic model. The hydrodynamics component uses Navier–Stokes equations for calculation of the incompressible flow in the water body velocity field and turbulent diffusion coefficients. The water quality component computes property sources and sinks, considering interactions between temperature, nutrients, algae, dissolved oxygen, organic matter, and sediments (Cole and Wells 2011).

Figure 2 illustrates the geometry used to describe the main Enxoé Reservoir areas and orientations, at full capacity, consisting of 12 segments with lengths of 150–350 m and widths of 300–1000 m at the surface. A minimum of four vertical layers upstream, and a maximum of 17 layers near the dam, all 1 m high, were further considered. The depth information was defined based on available reservoir and wall geometry data, provided by the APA.

The model boundary conditions included: daily river inputs of nitrate, ammonia, orthophosphate, organic matter, total suspended solids, and oxygen, computed with SWAT (Brito et al. 2017a); daily weather data (air temperature, humidity, wind velocity and direction, and cloud cover), from the nearest meteorological station (Herdade da Valada, located 4 km from the reservoir); reservoir outflow, computed from the reservoir balance between inflow, evaporation, and storage (Brito et al. 2017a); and the bottom internal load from sediments under anoxic conditions (mainly phosphorus).

The model simulations started in 2001 and ended in 2011. Initial conditions (reservoir level and nutrient, suspended sediment, algal and oxygen concentrations) were obtained from measured data. Initial concentrations were assumed to be homogeneous with depth (simulations started in winter), consistent with measured data.

Daily weather data was used in the model simulations, since hourly records showed frequent gaps; however, since wind gusts with high intensity for long periods can have a strong effect on the dismantling of stratification, daily averages of maximum hourly wind velocities were also used in CE-QUAL-W2 (sensitivity analysis then showed a better match between temperature predictions and field data, as opposed to using average hourly wind values). The dew point temperature was computed as follows Lawrence (2005):

$$T_d = T - (100 - RH)/5, \quad (1)$$

where T_d is the dew point temperature (°C), T is the air temperature (°C), and RH is the relative humidity (−). The first results showed consistent underestimation of winter minimum temperatures; dew point values were limited to a minimum of 10 °C or would very often drop to negative temperatures during winter that in turn would result in high evaporation and heat loss from the reservoir. In fact, a vertical air temperature gradient may have formed above the surface water, increasing temperatures at night (in comparison with data from the meteorological station 4 km away), reducing evaporation and heat loss (Condie and Webster 1997). Thus, this phenomenon ended up being accounted for in CE-QUAL-W2 by imposing a limit to the dew point values, which was the variable directly used in the model for simulating evaporation.

CE-QUAL-W2 model calibration/evaluation

The CE-QUAL-W2 model was calibrated/validated for the period 2001–2011 (current situation). Following that,

different management scenarios, with reduced nutrient loads and changed reservoir geometries, were tested to assess the reservoir trophic level response.

The field data used for calibration/validation of the CE-QUAL-W2 model were: (1) hourly reservoir levels, provided by the APA for the period 2001–2011; (2) monthly reservoir surface concentrations (nitrate, ammonia, orthophosphate, chlorophyll-*a*, oxygen, suspended solids), provided by the APA for the period 2001–2011 (2017); and (3) measured seasonal profiles of temperature, oxygen, turbidity, and pH, as well as Secchi disc measurements, collected for this study, for the period August 2009 to March 2012.

Both qualitative and quantitative measures of uncertainty were used to compare observed data with predicted values. Graphical analyses, such as time-series plots, were used to identify general trends, potential sources of error, and differences between measured and predicted values. The CE-QUAL-W2 model performance was further depicted by mean values, standard deviations, correlations, and the root-mean-squared error (RMSE), given by:

$$\mathrm{RMSE} = \frac{\sum_{i=i}^{n} \left(O_i - S_i\right)^2}{n}, \tag{2}$$

where O_i is the observed data, S_i is the simulated data, and n is the total number of data records. RMSE values close to zero indicate only small errors in the estimates and good model predictions. Taylor diagrams were also used for graphical representation of model performance (2001).

Model evaluation included the comparison of model predictions with respective measurements of daily reservoir water levels, and monthly concentrations of nitrate, total suspended solids, orthophosphate, chlorophyll-*a*, and dissolved oxygen. Model calibration procedures involved modifying a set of parameters (listed in Table 2 and mapped in Fig. 3) until deviations between the model predictions and the observations were minimized. These included changing algal growth rates and optimum temperatures for the different species, reducing extinction coefficients that control light availability at deeper depths, and reducing suspended sediment sinking rates. The calibrated parameters were thus modified to best fit measures of: (1) suspended sediment, by reducing sinking rates, justified by measured shallow suspended sediment concentrations, representative of very fine material, consistent with wind-driven resuspension in shallow-depth reservoirs, such as Enxoé; (2) algal blooms and oxygen depletion, by adapting algal growth rates and internal phosphorus loads; and (3) temperature profiles, by adjusting extinction coefficients.

CE-QUAL-W2 simulated the internal sediment phosphorus load under anoxic conditions (desorption) with a zero-order reaction, based on sediment oxygen demand (SOD; mgO_2 m^{-2}) and bottom-water oxygen availability. The model also simulated oxic sediment organic matter mineralization, with a first-order reaction in which organic matter input to the sediment was accounted for. To parameterize the zero-order anoxic release of phosphorus into the current scenario, the order of magnitude of the internal phosphorus load was estimated, based on MOHID-Land results (Brito et al. 2017b). As explained above, this represents a value three times higher than the annual estimated SWAT load. (Flood loads carrying phosphorus adsorbed into sediments would contribute an extra 1.2 tonP $year^{-1}$ to the reservoir.) The reservoir balance showed that half of the suspended solids input from the watershed (that transport the adsorbed phosphorus) were deposited, while the remainder exited the reservoir. As such, the estimate of annual internal phosphorus load (deposited phosphorus from flood loads) was considered to be 0.6 tonP $year^{-1}$ (half of the flood load contribution), being similar to the phosphorus load entering from the river (0.6 tonP $year^{-1}$ estimated by the SWAT model). The CE-QUAL-W2 SOD phosphorus fraction (Table 2) was adjusted accordingly, and only with this order of internal phosphorus load the model was able to represent the field data magnitude for the current scenario, suggesting that the internal load computed was realistic. One should be reminded that CE-QUAL-W2 dynamically computes the effective phosphorus release, based on the SOD and effective bottom-water oxygen concentration. Thus, for case scenarios where the reservoir is able to recover from the eutrophic state, and oxygen near the bottom increases, the phosphorus internal load would be reduced accordingly, and the model should be able to reproduce those effects.

Some inconsistencies were found in CE-QUAL-W2 when modelling oxygen reaction limitations, resulting in oxygen profiles that tended rapidly to zero, below the thermocline. The code was then modified to overcome these inconsistencies. CE-QUAL-W2 nitrification's dependence on oxygen follows a Monod-type relationship, described as:

$$\mathrm{DOfNit} = \frac{\mathrm{O_2}}{\mathrm{O_2} + \mathrm{KDO}}, \tag{3}$$

where DOfNit (−) is the dissolved oxygen fraction to be multiplied by the nitrification rates, KDO (mg L^{-1}) is the half-saturation dissolved oxygen concentration, and O_2 is the water dissolved oxygen (mg L^{-1}); however, for organic matter decay and algal respiration, this relationship was replaced by an ON/OFF switch so that only when oxygen concentrations neared zero the mineralization rates were switched off (oxygen factor is zero). Above zero, oxygen concentration mineralization was not dependent on, or limited by, oxygen (factor is always one):

$$\mathrm{DOfMinEx} = \begin{cases} 1 & \text{if} \quad \mathrm{DO} \geq 1\mathrm{E}-10 \\ 0 & \text{if} \quad \mathrm{DO} < 1\mathrm{E}-10 \end{cases}, \tag{4}$$

Table 2 CE-QUAL-W2 parameters for the Enxoé Reservoir

#	Parameter	Description	Default value	Calibrated value
1	AG #1	Algal growth rate for diatoms (day^{-1})	0.3–3.0	1
2	AG #2	Algal growth rate for chlorophyceae (day^{-1})	0.7–9.0	3
3	AG #3	Algal growth rate for cyanobacteria (day^{-1})	0.5–11	2.5
4	AT1 #1	Algal minimum temperature for diatoms (°C)	5	5
5	AT1 #2	Algal minimum temperature for chlorophyceae (°C)	5	12
6	AT1 #3	Algal minimum temperature for cyanobacteria (°C)	5	15
7	AT2 #1	Algal first optimum temperature for diatoms (°C)	25	10
8	AT2 #2	Algal first optimum temperature for chlorophyceae (°C)	25	15
9	AT2 #3	Algal first optimum temperature for cyanobacteria (°C)	25	23
10	AT3 #1	Algal last optimum temperature for diatoms (°C)	35	22
11	AT3 #2	Algal last optimum temperature for chlorophyceae (°C)	35	26
12	AT3 #3	Algal last optimum temperature for cyanobacteria (°C)	35	26
13	AT4 #1	Algal maximum temperature for diatoms (°C)	40	24
14	AT4 #2	Algal first maximum temperature for chlorophyceae (°C)	40	29
15	AT4 #3	Algal first maximum temperature for cyanobacteria (°C)	40	29
16	AR #1	Maximum dark algal respiration rate for diatoms (day^{-1})	0.04/0.01–0.59	0.03
17	AR #2	Maximum dark algal respiration rate for chlorophyceae (day^{-1})	0.04/0.01–0.59	0.03
18	AR #3	Maximum dark algal respiration rate for cyanobacteria (day^{-1})	0.04/0.01–0.59	0.03
19	AE #1	Maximum excretion rate for diatoms (day^{-1})	0.04/0.014–0.044	0.03
20	AE #2	Maximum excretion rate for chlorophyceae (day^{-1})	0.04/0.014–0.044	0.03
21	AE #3	Maximum excretion rate for cyanobacteria (day^{-1})	0.04/0.014–0.044	0.02
22	AM #1	Maximum mortality rate for diatoms (day^{-1})	0.1	0.05
23	AM #2	Maximum mortality rate for chlorophyceae (day^{-1})	0.1	0.02
24	AM #3	Maximum mortality rate for cyanobacteria (day^{-1})	0.1	0.02
25	AS #1	Settling velocity for diatoms (m day^{-1})	0.1/0.2	0.1
26	AS #2	Settling velocity for chlorophyceae (m day^{-1})	0.1/0.1	0.1
27	AS #3	Settling velocity for cyanobacteria (m day^{-1})	0.1/< 0–0.05	-0.1
28	EX SS	Extinction coefficient for suspended solids (m^{-1})	0.1	0.01
29	EX OM	Extinction coefficient for organic matter (m^{-1})	0.1	0.01
30	EX ZOO	Extinction coefficient for zooplankton (m^{-1})	0.1	0.01
31	BETA	Fraction of incident solar radiation absorbed at the water surface (%)	0.45	0.45
32	SSS	Suspended solids settling rate (m day^{-1})	1	0.01
33	POMS	POM settling rate (m day^{-1})	0.001–20	0.25
34	LDOMDK	Labile DOM decay rate (day^{-1})	0.1/0.01–0.64	0.12
35	RDOMDK	Refractory DOM decay rate (day^{-1})	0.001/0.0001–0.0064	0.002
36	LPOMDK	Labile POM decay rate (day^{-1})	0.08/0.001–0.1	0.08
37	RPOMDK	Refractory POM decay rate (day^{-1})	0.001/0.001–0.1	0.02
38	DO1	Dissolved oxygen concentration limitation curve first point (mg L^{-1})	–	1E−5
39	DO2	Dissolved oxygen concentration limitation curve second point (mg L^{-1})	–	5.0
40	DOK1	Dissolved oxygen limitation fraction first point	–	0.1
41	DOK2	Dissolved oxygen limitation fraction second point	–	0.99
42	ZG	Zooplankton maximum growth rate (day^{-1})	1.5	0.19
43	ZR	Zooplankton maximum respiration rate (day^{-1})	0.1	0.1
44	ZM	Zooplankton maximum mortality rate (day^{-1})	0.01	0.01
45	PO4R,	Anoxic orthophosphate release fraction of SOD (−)	0.001/0.03–0.15	0.05
46	NH4R	Anoxic ammonia release fraction of SOD (−)	0.001/0.05–0.15	0.037
47	SOD	Sediment oxygen demand ($gO_2\ m^{-2}\ day^{-1}$)	0.1–1.0	0.1
48	AERATION	Aeration method	LAKE 6	LAKE 6
49	NH4DK	Ammonium decay rate (day^{-1})	0.001–0.95	0.15

Table 2 (continued)

#	Parameter	Description	Default value	Calibrated value
50	NO3DK	Nitrate decay rate (day^{-1})	0.03/0.05–0.15	0.7

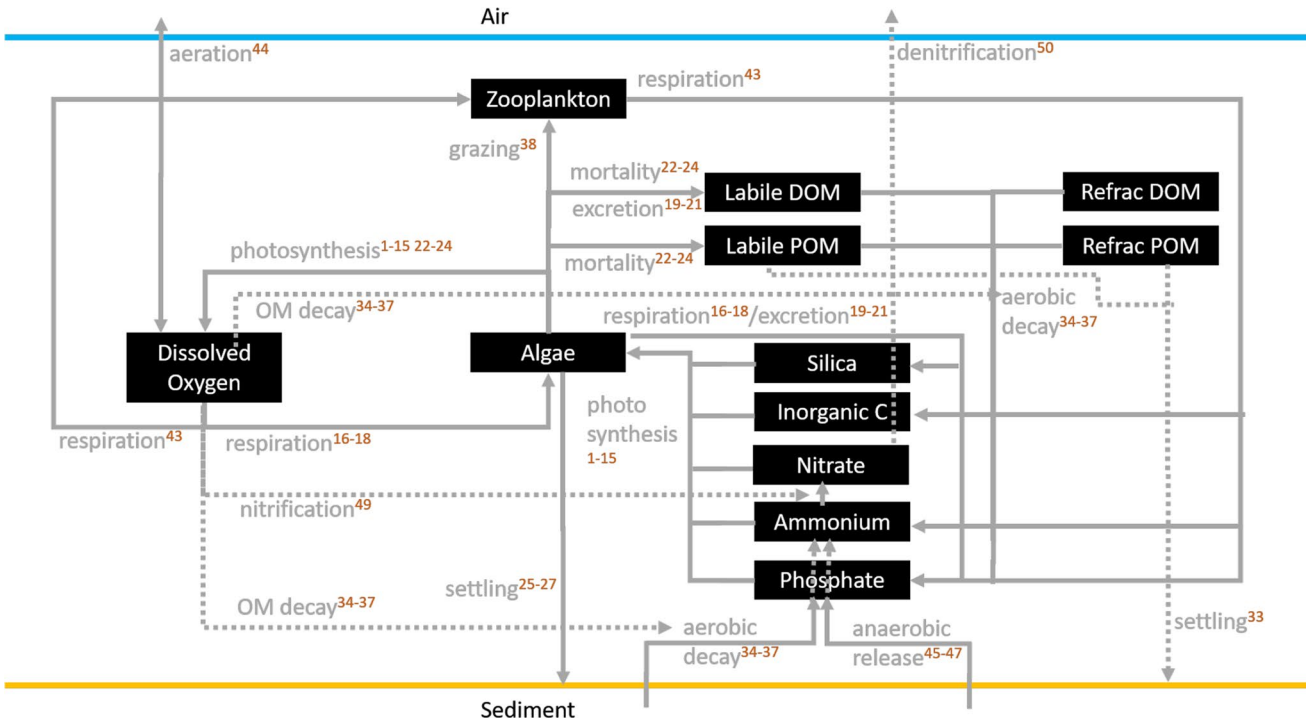

Fig. 3 CE-QUAl-W2 predominant water quality state variables (black boxes), and processes (arrows), with the definition of parameter numbers (orange) associated with each process (see Table 2)

where DOfMinEx (−) is the dissolved oxygen fraction to be multiplied by mineralization and algal excretion rates, and DO is the dissolved oxygen concentration (mg L^{-1}); however, this formulation is not generally used in water quality models, as in the examples of the WASP model (EPA 2009), or the ERSEM model (Butenschön et al. 2016), wherein Monod-type oxygen limitations are used. The original formulation in CE-QUAL-W2 meant that the Enxoé modelled dissolved oxygen profiles in summer tended rapidly to zero, just below thermocline (no surface exchange), despite all efforts to reduce it (see 'Result and discussion' section). On the other end, dissolved oxygen field data profiles were asymptotic to bottom-water minimum oxygen concentrations, which ranged from 1 to 3 mgO_2 L^{-1}. Therefore, the CE-QUAL-W2 model v3.7 code was changed so that all oxygen limitations could be defined by two points, each with an oxygen concentration and a fraction between zero and one, similarly to the CE-QUAL-W2 temperature rate multipliers:

$$\mathrm{DOAux} = \mathrm{DOK1} * \mathrm{EXP}\left[\frac{\mathrm{LOG}\left(\frac{\mathrm{DOK2}*(1.0-\mathrm{DOK1})}{\mathrm{DOK1}*(1.0-\mathrm{DOK2})}\right)}{(\mathrm{DO2}-\mathrm{DO1})*(\mathrm{DO}-\mathrm{DO1})}\right] \quad (5)$$

$$\mathrm{DOf} = \frac{\mathrm{DOAux}}{1+\mathrm{DOAux}-\mathrm{DOK1}}, \quad (6)$$

where DOf (−) is the dissolved oxygen fraction to be multiplied by rates, DO (mg L^{-1}) is the dissolved oxygen concentration, DO1 (mg L^{-1}) and DO2 (mg L^{-1}) are the two dissolved oxygen concentration points, and DOK1 (−) and DOK2 (−) are the respective limitation fractions. The latter formulation made the oxygen limitation uniform for all processes (mineralization, nitrification, and algal respiration) and combined with the parameters defined in Table 2, allowed for the modelled oxygen profiles in summer to 'detach' from zero below the thermocline, producing a similar asymptotic behaviour to the field data. Results using both the original and modified formulations are presented below.

Management scenarios (MS)

Five scenarios were considered to further investigate the response of the Enxoé trophic level to different management options:

- *MS1* No change scenario. This was the 'control' scenario, with the same forcing as the current situation;
- *MS2* Nutrient load reduction scenario, with no watershed loads. This was a hypothetical scenario to depict the evolution of the reservoir, while considering only the internal sediment phosphorus load and verifying whether it could be enough to fuel the algal blooms;
- *MS3* Nutrient load reduction scenario, with a 50% reduction in watershed loads (nutrients, organic matter) and 50% reduction in phosphorus SOD fraction. This represented a 50% load reduction from the watershed, both during low waters and flood events;
- *MS4* Nutrient load reduction scenario, with a 50% reduction in watershed loads (nutrients, organic matter) and no sediment phosphorus load. This was similar to the previous one, but required, for instance, bottom aeration to avoid anoxia and a phosphorus internal load, even though this existed only in the bottom sediments;
- *MS5* Reservoir dam height increased by 1 m, without any reduction in loads. This scenario aimed to test the geometry effect on the trophic level.
- *MS6* Similar to above, with dam height increased by 2 m, without any reduction in loads. This scenario aimed to test the geometry effect on the trophic level.

The scenarios were run continuously, from the end of the current situation simulation, for 10 years forward, to depict how the reservoir would evolve, and how fast. The same forcing as the current situation (e.g. same meteorology) was used, except for the specific definitions of each scenario. For the last two scenarios, it was necessary to run the current situation again, since the vertical geometry was changed to include the increase in dam height. As there is no reservoir volume-elevation curve for the new elevations, and to maintain the surface area and surface fluxes, one and two layers (1 m each), with the same surface dimensions as the original ones, were added to the original reservoir geometry for simplification. The 2-m height increase resulted in a small increase in the inundated area, where all of the surface area would be inside the 100-m protected zone in the Enxoé Reservoir management plan (Resolution 167/2006).

Results and discussion

Reference situation

Figure 4 compares the model predictions of water temperature with the measured profiles near the Enxoé Reservoir dam (17 m deep at full storage), during selected time periods. In the summer months (June to August), a thermal stratification was clearly observed, with differences between surface and bottom temperatures reaching 10 °C (e.g. 24 August 2009, 23 June 2010, and 18 July 2011). The thermocline usually occurred around 4–8 m depth. During winter months, stratification disappeared, due to lower air temperatures and stronger winds. Homogeneous temperature profiles, with lower water temperatures, were then observed (e.g. 01 February 2010, 29 October 2011, and 25 November 2011).

Figure 4 further shows that the model results were able to describe both the winter homogeneous profiles and summer stratification, including the thermocline location. This means that CE-QUAL-W2 was able to represent the main temperature processes occurring in the reservoir, i.e. one main driver for water circulation in the reservoir.

Figure 5 shows the comparison between model predictions (for the original and modified versions of CE-QUAL-W2) of dissolved oxygen profiles and field measurements taken near the Enxoé Dam. The main seasonal patterns for dissolved oxygen were similar to those for temperature. In the summer months (June–August), stratification was observed, with the maximum difference between surface and bottom concentrations reaching 5–10 mg L^{-1} (e.g. 24 August 2009, 23 June 2010, and 18 July 2011). Oxygen changes were very pronounced in the thermocline at 4 m, due to the existence of bottom sink processes (mineralization, nitrification), which occurred as the capacity to oxygenate was reduced with depth. In the winter months, stratification disappeared, due to lower air temperatures and stronger winds. Homogeneous profiles were then observed, showing higher dissolved oxygen concentrations (e.g. 01 February 2010, 29 October 2011, and 25 November 2011).

Figure 5 further showed that model results were able to represent winter homogeneous profiles and summer stratified profiles; however, the model in the original formulation tended to underestimate dissolved oxygen near the bottom during the summer months. The first hypothesis was that it could be due to elevated decay processes occurring near the bottom (mineralization, nitrification), lack of algal production (depths were relatively too shallow), and increased deposition of surface oxygen during winter, instead of being lost or consumed.

Sensitivity tests were performed to test each of those hypotheses. The reduction in decay processes (reduction

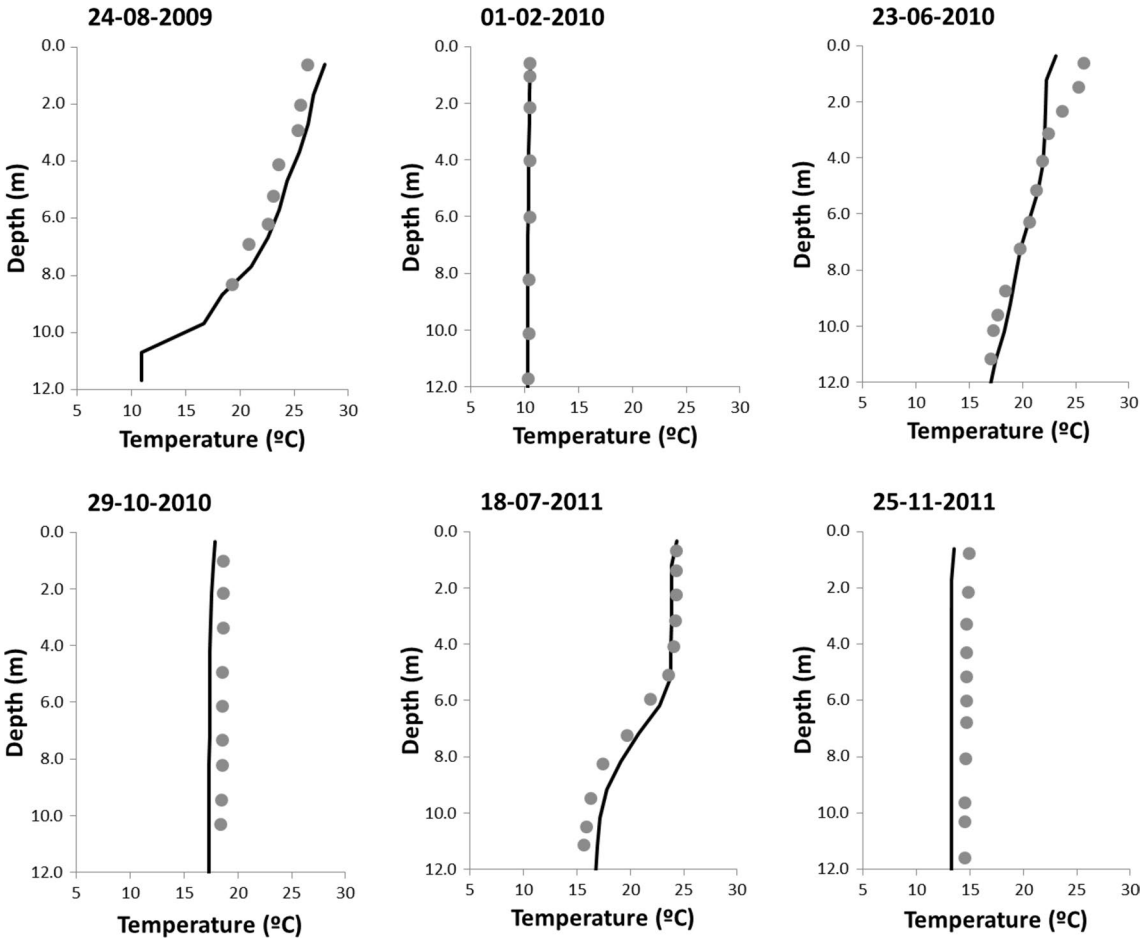

Fig. 4 Temperature profiles at the Enxoé Reservoir dam on different dates (model results—continuous black lines, field data—grey circles)

of mineralization and nitrification rates in the water column) improved the fit of oxygen levels near the bottom, but decreased the availability of nutrients and surface chlorophyll-*a* content, i.e. made the model underestimate organic matter in the reservoir.

Reducing extinction coefficients, or increasing sediment deposition (by reducing light attenuation), resulted in higher oxygen concentrations near the bottom (algae had more light available to start producing more oxygen), but the model started to deviate from measured surface suspended solids, or measured temperature profiles. The suspended solids registered very high concentrations in the reservoir (Fig. 6), and measured values were consistent with measured Secchi discs that showed minimum values of 1 m and maximum of 3 m. The Secchi disc data revealed that the photic zone was usually above/around the thermocline depth and that algae production was very limited below that depth, so not reasonably explaining the model's underestimation of oxygen in that zone.

Lastly, a parallel study, carried out using a Lagrangian vertical geometry, and the MOHID-Water model (Neves 2013), including the coupling with a CE-QUAL-W2 water quality model, showed reduced numerical diffusion, but did not improve the oxygen profile description either, until oxygen limitation was changed (unpublished work).

Only by considering the changes implemented in the CE-QUAL-W2 code (modified version), it was possible to 'detach' the bottom dissolved oxygen concentrations below the summer thermocline from zero, increasing oxygen availability, and better reproducing the field data.

Figure 6 presents the field measurements of water level, water temperature, TSS, nitrate, orthophosphate, chlorophyll-*a*, and dissolved oxygen content at the surface, near the reservoir dam, and compares these with the respective CE-QUAL-W2 model predictions (modified version) for the entire simulation period (2001–2011).

The measured and simulated water levels were very similar, which was expected, since the outflows were computed based on the reservoir balance. In the first years, the yearly level variation was only 1–2 m, but during 2004–2006 and 2008–2009, the reservoir level dropped to its minimum observed level (elevation around 170,

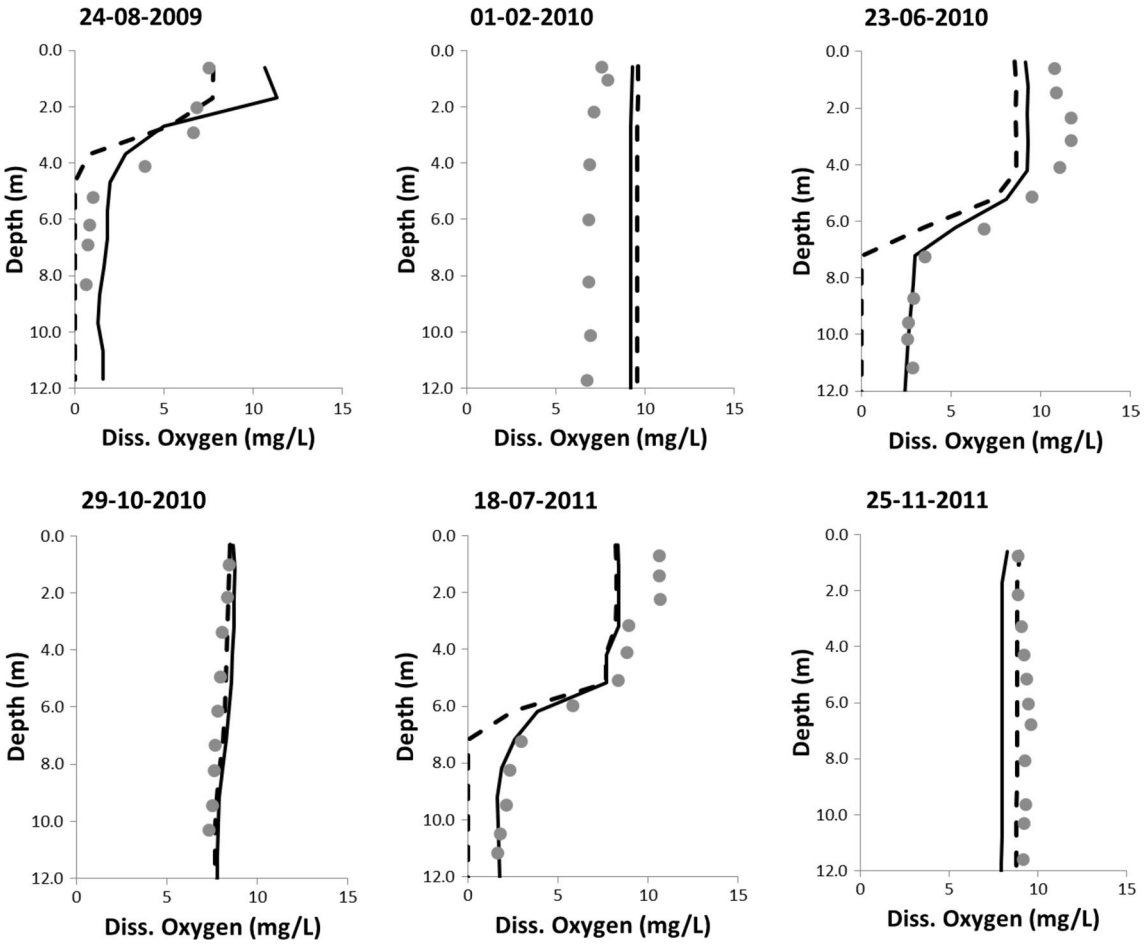

Fig. 5 Dissolved oxygen profiles at the Enxoé Reservoir dam on different dates (model results—continuous black line for modified CE-QUAL-W2 version, dashed line –original CE-QUAL-W2 version, field data—grey circles)

10 m depth near the dam), due to the extended droughts registered.

The measured surface water temperature ranged from 10 °C in winter to 25–30 °C in the summer. The model results were able to reproduce the minimum values, but at times overestimated the maximum temperature peaks. This overestimation was higher in years when the reservoir had higher water levels and can be related to an evaporative water-cooling effect, which increased with the surface area. That overestimation did not significantly influence the results, however, since both the field data values and overestimated modelled values were in the optimal temperature range for stimulating algal growth.

Measured surface TSS concentrations showed base values of 10 mg L^{-1} and peak values of up to 60–70 mg L^{-1}. The model estimations were able to represent the base values but underestimated the maximum peaks (the values went up to 30–40 mg L^{-1}) during high flow events. This can be related to the watershed flood transport process that occurs in just a few hours and is therefore difficult to describe with a daily time-step watershed model, such as SWAT (Brito et al. 2017b); however, as explained above, the missing input material ended up being implicitly included in the internal phosphorus load computation.

Measured surface nitrate concentrations were very low, ranging between 1 mg L^{-1} and the detection limit (0.5 mg L^{-1}). The model results were able to represent the range of variation of the field data, as well as the two higher peaks. These were coincident with the watershed inflows after drought years, which transported deposited material that had accumulated in the watershed.

Measured surface orthophosphate concentrations ranged between 0.02 and 0.1 mg L^{-1}. The model results showed a similar trend to the field data, being able to reproduce both minimum and maximum orders of values.

Total phosphorus is a good measure of not only the inorganic, but also the organic, material present in the reservoir. Measured values averaged 0.1 mg L^{-1}, and the model was able to get the order of magnitude of the field data, suggesting that the predicted organic load was also correct.

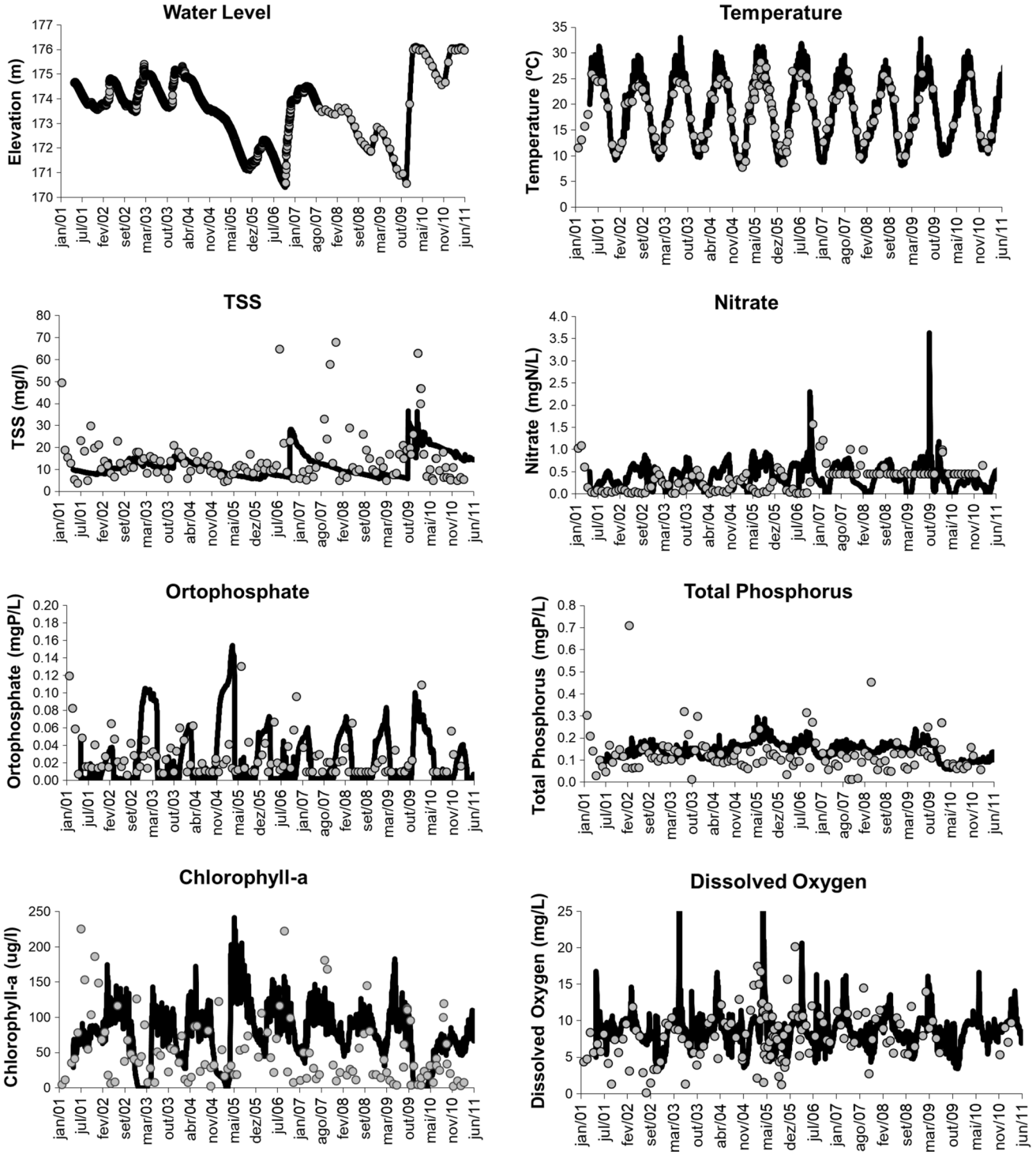

Fig. 6 Time-series of surface properties (water level, temperature, TSS, nitrate, orthophosphate, total phosphorus, chlorophyll-*a*, dissolved oxygen) at the Enxoé Reservoir dam on different dates (model results—continuous black line, field data—grey circles)

Measured surface chlorophyll-*a* concentrations registered minimum values on the order of units of ug L^{-1}, but were frequently above 50 ug L^{-1}, reaching maximum values above 200 ug L^{-1}. The modelled results were able to reproduce the maximum values and most of the minimum values, despite having a tendency to overestimate these (generally in winter). Three hypotheses were advanced: (1) autumn/winter algal growth was not limited enough; (2) the maximum rates for algal mortality, excretion, and respiration were underestimated; or (3) zooplankton grazing was

Table 3 Statistical analysis of measured field data and model estimates for the entire field data period (2001–2011)

Property	*N*	Data average	Data median	Data SD	Model average	Model median	Model SD	RMSE
Water level (m)	2349	173.6	173.8	1.2	173.5	173.7	1.2	0.04
Temperature (°C)	135	18.9	19.75	5.4	19.2	19.5	6.5	1.8
Dissolved oxygen (mg L^{-1})	141	8.2	8.0	3.4	12.1	10.6	5.6	7.6
Ammonia (mgN L^{-1})	114	0.3	0.17	0.38	0.23	0.2	0.15	0.4
Nitrate (mgN L^{-1})	117	0.34	0.41	0.28	0.39	0.34	04.27	0.4
Orthophosphate (mgP L^{-1})	116	0.32	0.15	0.39	0.02	0.003	0.03	0.48
Suspended solids (mg L^{-1})	126	14.7	11.5	11.4	18.9	19.3	6.34	13.65
Chlorophyll-*a* (µg L^{-1})	124	51.7	33.9	48.1	76.9	81.6	41.2	62.9

underestimated. Each of these hypotheses was tested. In terms of temperature limitation, increasing minimum algal temperatures affected algal growth globally (and not only during the measured minima); the temperatures calibrated for cyanobacteria were already adjusted to the higher spring/summer temperatures; and light limitation was not likely to be the problem, since the modelled temperature profiles showed good agreement with the measured ones (also at the surface), independently of the season, suggesting a correct light extinction estimation. After performing sensitivity tests on maximum algal mortality, excretion, and respiration, the model results showed that these processes globally affected the algal concentrations, and not only the minimum values. Finally, zooplankton growth effectively controlled algal decay, and specifically its minima, but testing higher growth rates produced long periods of very low algal concentrations (near zero) that were inconsistent with the field data. Thus, the current algae results represented the best possible results, with the model being able to reproduce the maximum values and main trends. This was essential for scenario testing, considering a water management perspective.

The modelled surface dissolved oxygen concentrations were well represented, including the oversaturation and intense production (reaching up to 20 mg L^{-1}) observed in the field data during algal blooms. The lower values (lower than 5 mg L^{-1}) were also simulated, in response to the oxidization of organic matter. Minimum concentrations were lower in the field data than in the model during the first few years. This was related to the differences found in algal (and organic matter) content between the field data and the model estimates. The algae decayed and consumed more oxygen in reality than in the model estimates, explaining the differences found in the minimum values; however, the model was able to reproduce most of the dissolved oxygen trends and its minima and maxima in the remaining years, showing that all key aspects for simulating this parameter were accounted for.

Overall, CE-QUAL-W2 was able to represent the main trend values of the properties that influence water circulation (water level and temperature). The model was further able to satisfactorily describe nutrient, algae, and dissolved oxygen trends, as well as the minimum and maximum values.

Table 3 and Fig. 7 present the statistical indicators obtained by comparing the model predictions with measured field data. The model estimates were of the same order of magnitude as the field data (similar average and median). Water level showed the best performance (high correlation value of 0.99, low RMSE value of 0.04 m, and similar deviation as the data), since outflows were computed to define the reservoir volume data. Temperature was also well predicted, with a high correlation value of 0.97 and small errors (less than 2 °C). Water quality results for nutrients, algae, and oxygen showed the worst statistical indicators, with RMSE values reaching 100% of the average values, and results deviating from the observed values in the Taylor's diagram (Fig. 7). This is a common behaviour in water quality simulations; while water temperature shows a typical seasonal variation, mainly due to solar radiation that is simulated straightforwardly, organic matter, nutrients, oxygen, and algae form a complex system that is often simplified in model formulations. Also, algal populations and individuals are usually lumped into functional groups to describe the main general processes and behaviours. As such, while the orders of magnitude of the values, minima and maxima could be reproduced, the exact timings were difficult to tackle, and a match between the field data and simulated values was difficult to reach.

The CE-QUAL-W2 model simulations were obtained after integrating the results from SWAT and were for a small reservoir of 10.4 hm^3. Nonetheless, the results were comparable with those reported from implementing CE-QUAL-W2 for large reservoirs, such as the 45,000-hm^3 Tucurui Reservoir in Brazil (Deus et al. 2013), or the 5900-hm^3 Karkheh Reservoir in Iran (Noori et al. 2015), and in medium-sized reservoirs, such as two reservoirs in Taiwan of 183 and 659 hm^3 (Kuo et al. 2006), or the 1400-hm^3 Shanmei Reservoir in China (Liu et al. 2015), where the ratio of RMSE to average values was below 0.6.

The measured trophic state (geometric average of chlorophyll-*a*) for the period 2001–2011 was 33 µg L^{-1}, while

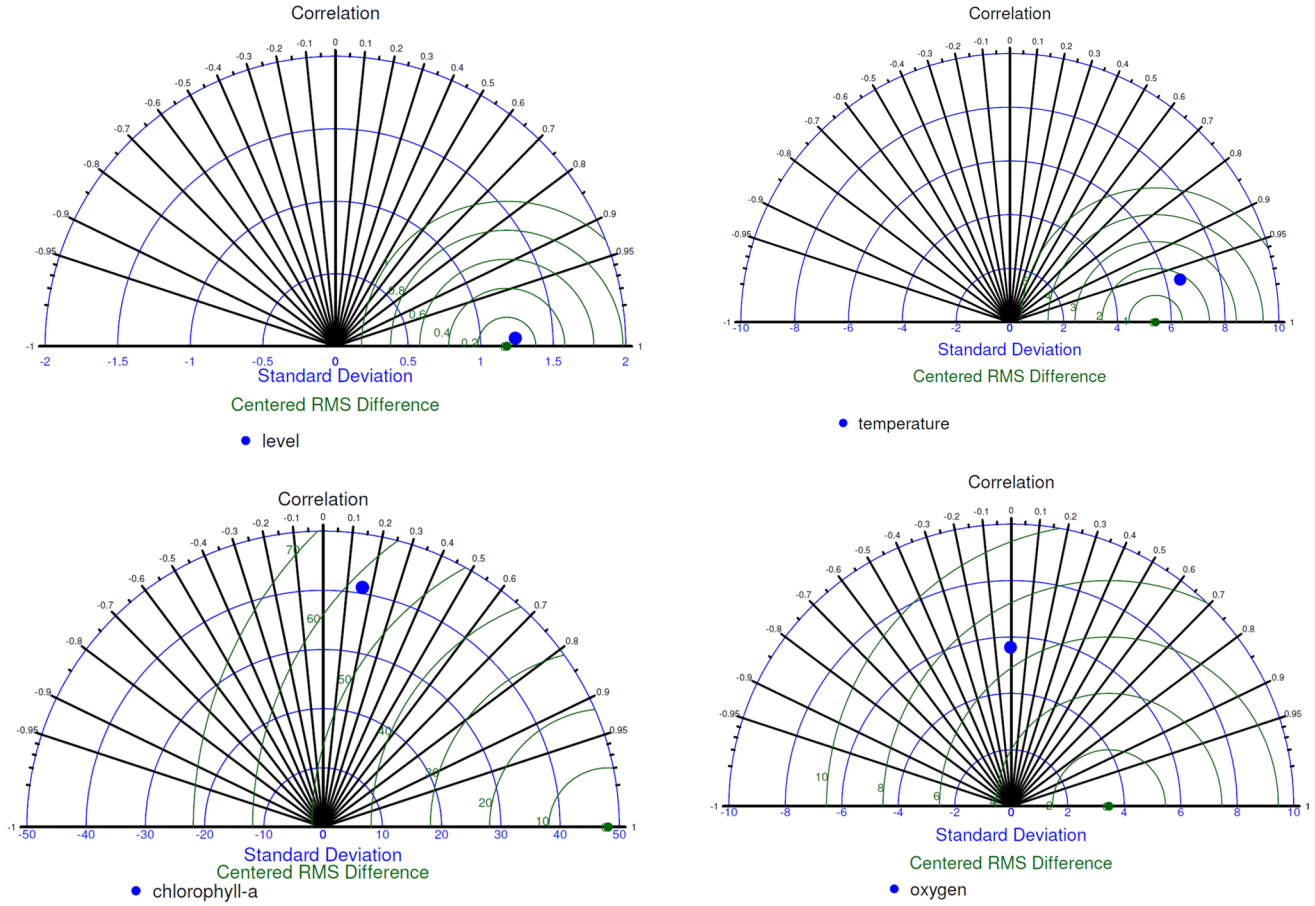

Fig. 7 Taylor diagrams for model fit for water level (top left), water temperature (top right), chlorophyll-*a* (bottom left), and dissolved oxygen (bottom right). The observed point (perfect fit) is represented by a green dot, and actual model result by a blue dot

Table 4 Vollernweider model for Enxoé in the current situation

Parameter	Unit	Computation	Value
Lake area (*A*)	m^2	–	2,050,000
Lake volume (*V*)	m^3	–	10,400,000
Lake discharge (*Q*)	$m^3\ yr^{-1}$	–	5,045,760
Hydraulic residence time (*T*)	yr	V/Q	2.06
Mean depth (*Z* mean)	m	–	5
Flushing rate	yr^{-1}	1/T	0.49
Total annual loading (*P* load)	$kg\ yr^{-1}$	–	1800
Water inflow (Wi)	m^3	–	6,622,560
Surface overflow rate (qs)	$m\ yr^{-1}$	*Z* mean/*T*	2.43
Total areal *P* loading (Lp)	$g\ m^{-2}\ yr^{-1}$	*P* load * 1E3/*A*	0.878
Vollenweider in-lake *P* concentration	$mg\ L^{-1}$ or $g\ m^{-3}$		0.149

the estimated value given by the model was 53 µg L^{-1} (both corresponding to eutrophy, since they were higher than the 10 µg L^{-1} defined as the national limit for eutrophication). The difference between the measured and predicted trophic state values returned around 60% of the measured value, but the difference between the measured and predicted averages of annual maximum chlorophyll-*a* values was less than 1% of the measured value. This is obviously important from a management standpoint, since algal blooms and maximum values are essential for water abstraction and treatment planning.

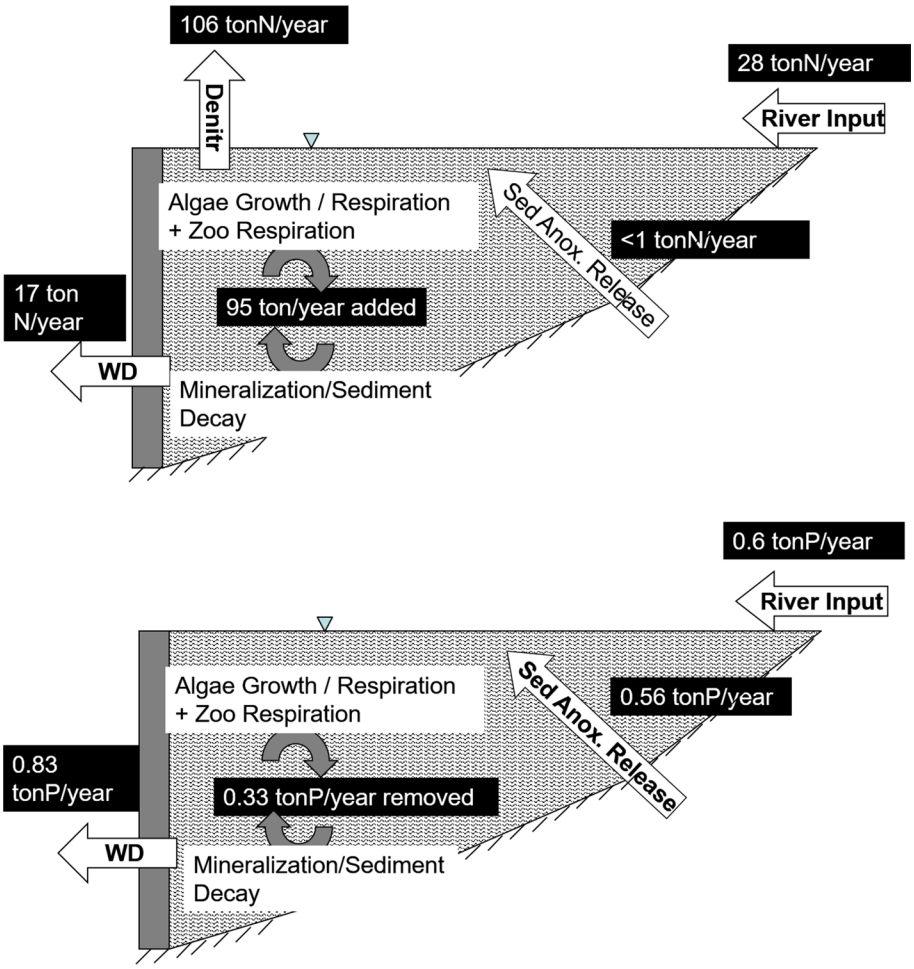

Fig. 8 Enxoé Reservoir nutrient budget: nitrogen (top) and phosphorus (bottom) fluxes. WD—water discharge

The CE-QUAL-W2 model results for the current situation were also compared to estimates using the Vollenweider and Kerekes model (1980) and expected reservoir phosphorus concentrations (Table 4). This model considered the physical characteristics of the reservoir (reservoir surface area, total volume, and average depth), the average inflows and outflows, and the total load (1.8 tonP year^{-1}, including external and internal sources). Results showed that the expected phosphorus concentration in the reservoir was 0.1 mgP L^{-1}, corresponding to the same order of measured and modelled maximum orthophosphate and average total phosphorus concentrations. Results of the Vollenweider model were thus consistent with Enxoé's eutrophic state and the CE-QUAL-W2 predictions.

The present integrated model was considered to be able to represent the main aspects of reservoir stratification (that influences the hydrodynamics) and long-term surface data. As such, the model was used to extrapolate results and predict the most effective management actions that could reduce the Enxoé Reservoir's trophic level.

Reservoir nutrient budgets

After model calibration and satisfactory simulation of the measured field data (surface and profiles), CE-QUAL-W2 was used to represent the Enxoé Reservoir budgets and to understand the main processes responsible for feeding its high trophic level.

Figure 8 shows the estimated average nitrogen and phosphorus annual fluxes in each component (river inflow, reservoir outflow, denitrification, algal assimilation/respiration, plus zooplankton respiration, sediment release under anoxic conditions, and organic matter decay, or mineralization) for the period 2001–2011. For nitrogen, 17 tonN year^{-1} (around 60% of the input) was routed outside the reservoir with outflow; a high level of nitrogen recycling existed, due to algal nitrogen assimilation/death, and consequent organic matter decay, including denitrification while under anoxic conditions (most part of summer). For phosphorus, 0.83 tonP year^{-1} (around 140% of the input) was routed outside the reservoir with outflow; almost 100% of the input (around 0.6 tonP year^{-1}) was generated from sediment bottom release; the internal phosphorus recycling

Table 5 Enxoé management scenarios maximum and average chlorophyll-*a* concentrations and respective reductions

Management scenario	Maximum[a] (ug L^{-1})	Reduction in maximum[b]	Average[a] (ug L^{-1})	Reduction in average[b]
Measured data—current situation	158	–	55	
Model CS—current situation	159	–	79	
Model MS1—no change to current situation	203 (120)	–	99 (66)	
Model MS2—removal of load in river in relation to current situation	176 (83)	13 (31) %	86 (46)	13 (30) %
Model MS3—reduction of 50% *P* load (river input + bottom sediment SOD *P* fraction) in relation to current situation	97 (54)	52 (55) %	52 (35)	47 (47) %
Model MS4—reduction of 50% *P* load in river + removal of sediment *P* load, in relation to current situation	44 (31)	78 (74) %	25 (21)	75 (68)
Model MS5—increase dam wall by 1 m (average depth 6 m, instead of 5 m)	186 (124)	8 (+ 3) %	88 (68)	11 (+ 3) %
Model MS6—increase dam wall by 2 m (average depth 7 m instead of 5 m)	34 (26)	83 (78) %	9.3 (11.8)	91 (82) %

[a]Values computed for 2002–2010 for current situation and hypothetical scenarios for eight following years. Maximum values are the average of annual maxima, last 2 years' values are presented in brackets

[b]Reduction in percentage for scenarios, in comparison with MS1

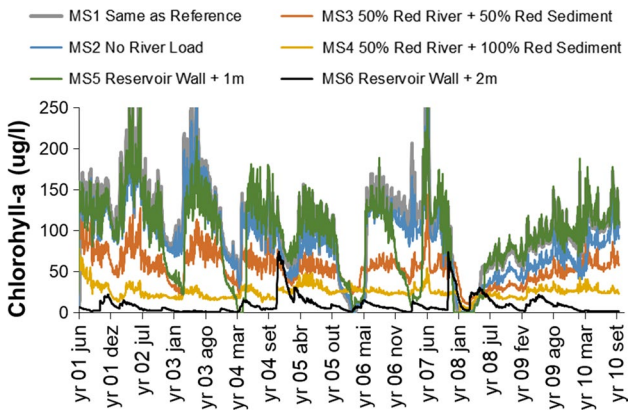

Fig. 9 Enxoé future scenarios for chlorophyll-*a* concentration

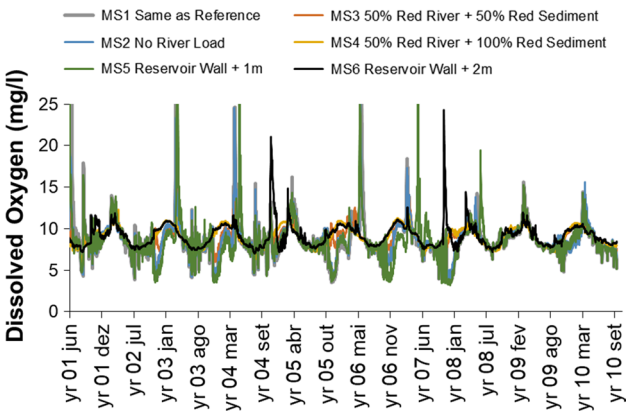

Fig. 10 Enxoé Reservoir future scenarios for dissolved oxygen

processes (algal assimilation, organic matter decay, or mineralization) removed around 55% of the phosphorus input (0.33 tonP $year^{-1}$).

The Enxoé Reservoir acted as a nutrient recycler between algal cycles, with reduced dependency on watershed inputs because of cyanobacteria dominance, which were able to assimilate atmospheric N_2, sustained by internal sediment phosphorus loads (of the same order as the watershed input). Søndergaard et al. (1992) also reported a relatively high sediment phosphorus release rate in Lake Arresø (Denmark) during resuspension because of the low Fe–P ratio and the type of sediment. The importance of internal phosphorus loading for reservoir water quality was further discussed by Søndergaard et al. (2003), who inferred that the internal phosphorus release contributing to a reservoir's high trophic level can last for several decades, even when external loading has been reduced.

Reservoir response to management scenarios

Table 5 presents the average and mean annual maximum chlorophyll-*a* concentrations of all the management scenarios considered, while Figs. 9 and 10 present the dam surface chlorophyll-*a* and oxygen time-series concentrations, respectively.

The MS1 scenario, which corresponded to a continuation of current conditions (used the same forcing as in the original current simulation), resulted in similar patterns and higher average and maximum concentrations, compared to the current situation. This constituted a base scenario for comparison of the remaining simulations. Nonetheless, the

Table 6 Vollernweider model for an Enxoé management scenario of 10-m increase in dam height

Parameter	Units	Computation	Value
Lake area (*A*)	m^2	–	2,050,000
Lake volume (*V*)	m^3	–	10,400,000
Lake discharge (*Q*)	$m^3\ yr^{-1}$	–	5,045,760
Hydraulic residence time (*T*)	yr	V/Q	2.06
Mean depth (*Z* mean)	m	–	15
Flushing rate	yr^{-1}	1/T	0.49
Total annual loading (*P* load)	$kg\ yr^{-1}$	–	1800
Water inflow (Wi)	m^3	–	6,622,560
Surface overflow rate (qs)	$m\ yr^{-1}$	*Z* mean/*T*	7.28
Total areal *P* loading (*L*p)	$g\ m^{-2}\ yr^{-1}$	*P* load * 1E3/*A*	0.878
Vollenweider in-lake *P* concentration	$mg\ L^{-1}$ or $g\ m^{-3}$		0.05

results showed that, in the case of similar forcing conditions, not changing the management could have a negative impact on the reservoir, further increasing the chlorophyll-*a* concentrations.

The MS2 scenario, which tested the dependence on internal load, showed reductions of 13% for average and maximum chlorophyll-*a* concentrations during the entire simulation period, in relation to MS1 (Table 5). These reductions were hardly noticeable over the years (Fig. 9), meaning that internal phosphorus loads were able to fuel algal blooms during the time period considered.

The MS3 scenario, with 50% phosphorus load reduction (from river input and the bottom sediment SOD fraction), led to a reduction of chlorophyll-*a* maximum and average concentrations between 47 and 52%, when compared to MS1.

The MS4 scenario, similar to MS3 with a 50% reduction from river input, but with the removal of the internal phosphorus load (e.g. by maintaining high dissolved oxygen levels at the bottom of the reservoir), resulted in a 75–78% reduction in the average and maximum chlorophyll-*a* concentrations, when compared to MS1. Applying this reduction to the current situation field data average (55 $\mu g\ L^{-1}$), the resulting average chlorophyll-*a* concentration values yielded 12–14 $\mu g\ L^{-1}$ (or geometric averages of 7–8 $\mu g\ L^{-1}$, as used in the national trophic status definition). Despite this, the achieved trophic level was still 30–40% above or below (considering average or geometric average values) the national level for eutrophication (10 $\mu g\ L^{-1}$), being difficult to sustain it as safe. Decreasing loads to these levels would require: (1) reducing the suspended material inflow to the reservoir (that is loaded with phosphorus), especially during flood events; and (2) removing anoxia from the reservoir bottom. The first management option could be accomplished by placing retention barriers upstream to retain sediment, by preserving riparian vegetation, which would partially use some of the nutrients exported to the river, before they reached the reservoir, or by promoting conservation tillage practices in the watershed (Hashemi et al. 2016). The second management option could be achieved by using oxygen aeration at the reservoir bottom. These results follow Marsden (1989), who pointed out that improvements in the condition of highly eutrophic lakes require very large reductions in external phosphorus loading.

The difficulty in reaching a safe trophic state in the Enxoé Reservoir, and the expected costly investment needed for implementing the latter scenarios, highlighted the need for an additional scenario to depict the relationship of the trophic state to the reservoir geometry. (Enxoé Reservoir has a 5-m average depth.) The Vollenweider model was applied to the dam wall increase scenarios, and only an increase of 10 m (average depth consequently increased to 15 m) would produce a mesotrophic level. The expected phosphorus concentration output, without considering any load reduction, reached 0.05 $\mu g\ L^{-1}$ (Table 6), representing a mesotrophic state (Vollenweider and Kerekes 1980). These results agreed generally with those from INAG (2009) and Mateus et al. (2014), who studied the trophic levels of 30 reservoirs in Portugal under the scope of the Waste Water Treatment Plant directive. They showed that, generally, reservoirs with mean depths of less than 10 m are eutrophic, even with low urban or diffuse loads. On the other hand, higher mean depths limited the summer phosphorus internal load from reaching the photic/algal production zone in most of the reservoirs, blocking the predominant mechanism for algal blooms in the absence of river inputs (low/absent inflows in summer). The same was found with the current study, with the breakpoint being a 7-m average depth. The reservoir wall increase of 1 m, to an average depth of 6 m (MS5), did not much improve the reservoir trophic state in relation to MS1, but for the 2-m wall increase and 7 m average depth (MS6), chlorophyll-*a* concentrations were reduced 82–91%, in relation to MS1. Applying this reduction to the current situation field data average (55 $\mu g\ L^{-1}$), the resulting average values yielded an average chlorophyll-*a* concentration of 5–10 $\mu g\ L^{-1}$ (or a geometric average of 3–6 $\mu g\ L^{-1}$),

representing a mesotrophic level, two times lower than the national eutrophication level.

The scenario's reductions were forced instantaneously (no smooth transition), and the trophic state reduction was linear with load reduction, over a 10-year period, when the phosphorus internal load was changed. On the other hand, the change in chlorophyll-*a* and dissolved oxygen concentrations was slow, and almost not noticeable, when only river external load was acted upon, even in the MS2 total removal scenario (Figs. 9 and 10).

Future studies should focus on: (1) integrating a full water quality watershed model, with an adsorbed phosphorus component, and a reservoir model with sediment diagenesis, to further detail the phosphorus pathways; and (2) cost–benefit analyses to determine the best management approaches, based on the current/further work proposed.

The management scenarios were intentionally set for testing extreme conditions. The best approach can likely be a mix of several management options. Since geometry changes are limited, approaches should also test how to reduce phosphorus load to the reservoir, particularly during flood events (e.g. managing erosion with agricultural practices or trapping sediment in ditches, etc.), and the feasibility of removing internal load from sediment. Future work should also take advantage of the integration strategy to assess where in the watershed the load reductions could be more effective.

Conclusions

This work presented a novel integrated modelling approach that coupled a watershed (SWAT) and a reservoir (CE-QUAL-W2) model to depict the origin of the Enxoé Reservoir trophic state—the highest in Portugal.

Previous modelling studies estimated nutrient loads from the watershed to the reservoir of 28 and 0.6 tonP year^{-1} for the period 2001–2011. Although these values can be considered relatively low, corresponding to similar values reported in the literature for extensive agricultural areas with gentle slopes (low erosion) and reduced human presence, short-term floods were found to be able to transport up to three times the average annual phosphorus load.

The integrated model results were compared with profile information collected over 2 years (temperature, oxygen), and surface properties measured during the entire reservoir lifetime (chlorophyll-*a*, nitrate, orthophosphate, suspended sediment, oxygen). The model was able to represent stratification formation, with spring–summer high temperatures, reduced inflows and wind, as well as its destruction with increased flow and wind velocity in winter. The model was further able to represent the thermocline depth (at around 4 m). The model was also satisfactorily fitted to the water surface data, in respect to nutrients, suspended sediment, oxygen, and chlorophyll-*a* concentrations.

The reservoir budget showed that phosphorus load from bottom sediments and nitrogen load from the atmosphere could fuel blooms, when nutrient input from the watershed was low. Also, internal recycling (algal and organic matter decay, and nutrient assimilation and decay) can sustain high algal concentrations for months. Since atmosphere nitrogen input is not controllable, the most effective options to control the reservoir trophic level are by controlling internal phosphorus load, or its geometry. The management scenarios showed that the internal sediment phosphorus load is vital for regulating the trophic state. Reducing the total phosphorus input by 75% (externally from watershed sources and internally from the bottom sediment source) could reduce the reservoir trophic level to close to the eutrophication limit, but only with a reservoir wall increase of 2 m (by limiting the phosphorus internal load's ability to reach the photic zone in parts of the reservoir) could sustain a mesotrophic state level.

Future studies should address phosphorus pathways in more detail (from a model development perspective) and produce cost–benefit analyses to compare the scenarios proposed, in order to depict the best approach for the reduction of trophic state and algal blooms in reservoirs (from a management perspective).

Acknowledgements This work was supported within the framework of the EU Interreg SUDOE IVB program (SOE1/P2/F146 AguaFlash project), the Project Mirage (EU-FP7), and the Project EUTROPHOS (PTDC/AGR-AAM/098100/2008) of the Fundação para a Ciência e a Tecnologia (FCT). MARETEC acknowledges the national funds from the FCT (Project UID/EEA/50009/2013). TBR was supported by FCT grant SFRH/BPD/110655/2015.

References

APA (2017) Analytical techniques for water quality parameters, ARH-Alentejo laboratories. 2017. From http://apambiente.pt/_zdata/LRA/Parametros_Metodos_ARHALT_Site_2017.pdf. Accessed Aug 2017. In Portuguese

Brito D, Neves R, Branco MA, Prazeres Â, Rodrigues S, Gonçalves MC, Ramos TB (2017a) Assessing water and nutrient long-term dynamics and loads to an eutrophic reservoir in the Enxoé temporary river basin, southeast Portugal. Appl Water Sci (In review)

Brito D, Neves R, Branco MA, Gonçalves MC, Ramos TB (2017b) Modeling flood dynamics in a temporary river basin draining to an eutrophic reservoir in southeast Portugal. Environ Earth Sci 76:377

Butenschön M, Clark J, Aldridge JN, Allen JI, Artioli Y, Blackford J, Bruggeman J, Cazenave P, Ciavatta S, Kay S, Lessin G, van Leeuwen S, van der Molen J, de Mora L, Polimene L, Sailley S, Stephens N, Torres R (2016) ERSEM 15.06: a generic model for marine biogeochemistry and the ecosystem dynamics of the lower trophic levels. Geosci Model Dev 9:1293–1339

Coelho H, Silva A, Chambel-Leitão P, Obermann M (2008) On the origin of cyanobacteria blooms in the Enxoé reservoir. In: 13th world water congress, international water resources association, Montpellier, France

Cole TM, Wells SA (2011) CE-QUAL-W2: a two-dimensional, laterally averaged, hydrodynamic and water quality model, Version 3.71. User manual. U.S. Army Corps of Engineers, Washington, DC, 20314-1000

Condie SA, Webster IT (1997) The influence of wind stress, temperature, and humidity gradients on evaporation from reservoirs. Water Resour Res 33(12):2813–2822

Debele B, Srinivasan R, Parlange J-Y (2008) Coupling upland watershed and downstream waterbody hydrodynamic and water quality models (SWAT and CE-QUAL-W2) for better water resources management in complex river basins. Environ Model Assess 13:135–153. https://doi.org/10.1007/s10666-006-9075-1

Dechmi F, Burguete J, Skhiri A (2012) SWAT application in intensive irrigation systems: model modification, calibration and validation. J Hydrol 470–471:227–238. https://doi.org/10.1016/j.jhydrol.2012.08.055

Deus R, Brito D, Mateus M, Isabella K, Fornaro A, Neves R, Alves CN (2013) Impact evaluation of a pisciculture in the Tucuruí reservoir (Pará, Brazil) using a two-dimensional water quality model. J Hydrol 487:1–12

EPA (2009) WASP7 Stream transport model theory and user's guide supplement to Water Quality Analysis Simulation Program (WASP) user documentation

Gassman PW, Reyes MR, Green CH, Arnold JG (2007) The soil and water assessment tool: historical development, applications, and future research directions. Trans ASABE 50(4):1211–1250. https://doi.org/10.13031/2013.23637

Geza M, McCray JE (2008) Effects of soil data resolution on SWAT model stream flow and water quality predictions. J Environ Manag 88(3):393–406. https://doi.org/10.1016/j.jenvman.2007.03.016

Green CH, van Griensven A (2008) Autocalibration in hydrologic modeling: using SWAT2005 in small-scale watersheds. Environ Model Soft 23:422–434

Hashemi F, Olesen JE, Dalgaard T, Børgesen CD (2016) Review of scenario analyses to reduce agricultural nitrogen and phosphorus loading to the aquatic environment. Sci Total Environ 573:608–626

Havens KE, James RT, East TL, Smith VH (2003) N: P ratios, light limitation, and cyanobacterial dominance in a subtropical lake impacted by non-point source nutrient pollution. Environ Poll 122:379–390

INAG (2004) Plano de Ordenamento da Albufeira do Enxoé, estudos de caracterização e pré-proposta de ordenamento. Instituto da Água, MAOTDR, Lisbon

INAG (2009) Management of the Trophic Status in Portuguese Reservoirs. Report on classification and trophic state reduction in the scope of WWTP Directive. Instituto da Água. Lisbon

INE (2001) Recenseamento Geral Agrícola. Instituto Nacional de Estatística, Lisbon

Kuo JT, Lung WS, Yang CP, Liu WC, Yang MD, Tang TS (2006) Eutrophication modelling of reservoirs in Taiwan. Environ Model Soft 21(6):829–844

Kurup RG, Hamilton DP, Phillips RL (2000) Comparison of two 2-dimensional, laterally averaged hydrodynamic model applications to the Swan River Estuary. Math Comp Simul 51(6):627–638

Lawrence MG (2005) The relationship between relative humidity and the dew point temperature in moist air: a simple conversion and applications. Bull Am Meteorol Soc 86:225–233

Liu M, Chen X, Yao H, Chen Y (2015) A coupled modeling approach to evaluate nitrogen retention within the Shanmei Reservoir watershed, China. Estuar Coastal Shelf Sci 166:189–198

Lung WS, Bai S (2003) A water quality for the patuxent estuary: current conditions and predictions under changing land-use scenarios. Estuaries 26:267–279

Makinia J, Wells S, Zima P (2005) Temperature modeling in activated sludge systems: a case study. Water Environ Res 77(5):525

Marsden MW (1989) Lake restoration by reducing external phosphorus loading: the influence of sediment phosphorus release. Freshw Biol 21:139–162

Martin N, McEachern P, Yu T, Zhu DZ (2013) Model development for prediction and mitigation of dissolved oxygen sags in the Athabasca River, Canada. Sci Total Environ 443:403–412

Mateus M, Almeida C, Brito D, Neves R (2014) From eutrophic to mesotrophic: modelling watershed management scenarios to change the trophic status of a reservoir. Int J Environ Res Public Health 11(3):3015–3031

Neitsch SL, Arnold JG, Kiniry JR, Srinivasan R, Williams JR (2002) Soil and water assessment tool. User's Manual. Version 2005. GSWRL Report 02-02, BRC Report 2-06, Temple, Texas, USA

Neves R (2013) The MOHID concept. In: Mateus M, Neves R (eds) Ocean modelling for coastal management e case studies with MOHID. IST Press, Lisbon, pp 1–11

Noori R, Yeh HD, Ashrafi K, Rezazadeh N, Bateni SM, Karbassi A, Kachoosangi FT, Moazami S (2015) A reduced-order based CE-QUAL-W2 model for simulation of nitrate concentration in dam reservoirs. J Hydrol 530:645–656

Paerl HW, Fulton RS, Moisander PH, Dyble J (2001) Harmful freshwater algal blooms: with an emphasis on cyanobacteria. Sci World J 1:76–113

Panagopoulos Y, Makropoulos C, Mimikou M (2011) Reducing surface water pollution through the assessment of the cost-effectiveness of BMPs at different spatial scales. J Environ Manag 92(10):2823–2835

Ramos TB, Gonçalves MC, Branco MA, Brito D, Rodrigues S, Sánchez-Pérez JM, Suavage S, Prazeres A, Martins JC, Fernandes ML, Pires FP (2015a) Sediment and nutrient dynamics during storm events in the Enxoé temporary river, southern Portugal. CATENA 127:177–190. https://doi.org/10.1016/j.catena.2015.01.001

Ramos TB, Rodrigues S, Branco MA, Prazeres A, Brito D, Gonçalves MC, Martins JC, Fernandes ML, Pires FP (2015b) Temporal variability of soil organic carbon transport in the Enxoé agricultural watershed. Environ Earth Sci 73:6663–6676. https://doi.org/10.1007/s12665-014-3888-z

Rolff C, Almesjo L, Elmgren R (2007) Nitrogen fixation and abundance of the diazotrophic cyanobacterium *Aphanizomenon* sp. in the Baltic Proper. Marine Eco Prog Ser 332:107–118

Søndergaard M, Kristensen P, Jeppesen E (1992) Phosphorus release from resuspended sediment in the shallow and wind-exposed Lake Arresø, Denmark. Hydrobiologia 228:91–99

Søndergaard M, Jensen JP, Jeppesen E (2003) Role of sediment and internal loading of phosphorus in shallow lakes. Hydrobiologia 506(1–3):135–145

Taylor KE (2001) Summarizing multiple aspects of model performance in a single diagram. J Geophys Res 106:7183–7192

Valério E (2008) Molecular approaches in cyanobacteria: from detection and diversity to DNA-Based Biosensors. Ph.D. Thesis, Faculdade de Ciências, University of Lisbon

Valério E, Pereira P, Saker ML, Franca S, Tenreiro R (2005) Molecular characterization of Cylindrospermopsis raciborskii strains isolated from Portuguese freshwaters. Harmful Algae 4:1044–1052

Vollenweider RA, Kerekes JJ (1980) Background and summary results of the OECD cooperative program on eutrophication. In: Proceedings of an international symposium on inland waters and lake restoration. U.S. environmental protection agency. EPA 440/5-81-010. pp 26–36

Xu Z, Godrej NA, Grizzard TJ (2007) The hydrological calibration and validation of a complexly-linked watershed–reservoir model for the Occoquan watershed, Virginia. J Hydrol 3–4:167–183

Yevenes MA, Mannaerts CM (2011) Seasonal and land use impacts on the nitrate budget and export of a mesoscale catchment in Southern Portugal. Agric Water Manag 102:54–65

Zhang X, Srinivasan R, Van Liew M (2008) Multi-site calibration of the SWAT model for hydrologic modeling. Trans ASABE 51(6):2039–2049